Phylogenetic Articulation of Uric Acid Evolution in Mammals and How It Informs a Therapeutic Uricase

Ze Li, Yosuke Hoshino, Lily Tran, and Eric A. Gaucher*

Department of Biology, Georgia State University, Atlanta, GA, USA

*Corresponding author: E-mail: egaucher@gsu.edu.

Associate editor: Fabia Ursula Battistuzzi

Abstract

The role of uric acid during primate evolution has remained elusive ever since it was discovered over 100 years ago that humans have unusually high levels of the small molecule in our serum. It has been difficult to generate a neutral or adaptive explanation in part because the uricase enzyme evolved to become a pseudogene in apes thus masking typical signals of sequence evolution. Adding to the difficulty is a lack of clarity on the functional role of uric acid in apes. One popular hypothesis proposes that uric acid is a potent antioxidant that increased in concentration to compensate for the lack of vitamin C synthesis in primate species ~65 Ma. Here, we have expanded on our previous work with resurrected ancient uricase proteins to better resolve the reshaping of uricase enzymatic activity prior to ape evolution. Our results suggest that the pivotal death-knell to uricase activity occurred between 20 and 30 Ma despite small sequential modifications to its catalytic efficiency for the tens of millions of years since primates lost their ability to synthesize vitamin C, and thus the two appear uncorrelated. We also use this opportunity to demonstrate how molecular evolution can contribute to biomedicine by presenting ancient uricases to human immune cells that assay for innate reactivity against foreign antigens. A highly stable and highly catalytic ancient uricase is shown to elicit a lower immune response in more human haplotypes than other uricases currently in therapeutic development.

Key words: **uricase, uric acid, ancestral sequence reconstruction, ancient protein, mammalian evolution, gout therapeutics.**

Introduction

Uric acid is a small molecule generated mostly by purine metabolism that is subsequently excreted by host organisms after it is oxidized to soluble molecules. The concentration of endogenous uric acid levels are controlled by enzymes upstream and downstream of uric acid in its metabolic pathway, as well as membrane transporters of the small molecule (Ramazzina et al. 2006; Keebaugh and Thomas 2010). This control is important because uric acid becomes insoluble and forms crystalloids at increasing concentrations, which can quickly cause renal failure in mammals (Kelly et al. 2001). Even sustained moderate levels of uric acid can also cause crystals to accumulate in avascular tissue (e.g., cartilage, tendons, ligaments) and lead to long-term complications such as gout (Hershfield et al. 2010).

Apes are unique among nearly all other mammals because they have modified their control of endogenous uric acid levels (Wells 1910). In particular, apes lack a functional form of the enzyme uricase that would otherwise oxidize uric acid. Further, uric acid membrane transporters in ape kidneys have evolved to reabsorb most of the uric acid from the urine at normal physiological conditions and return it back to the blood, while those of nonapes have evolved to excrete most of the small molecule as waste. An evolutionary explanation for modifying the flux of uric acid has remained elusive (Kratzer et al. 2014).

Uric acid is recognized as an antioxidant and considered to be one of the most important antioxidants in the plasma (Ames et al. 1981), although its role in oxidative stress has been disputed (Hershfield et al. 2010). One popular hypothesis posits that the endogenous uric acid observed in apes evolved as a compensation for the lack of vitamin C synthesis in primates (Ames et al. 1981). It is generally regarded that primates lost the ability to synthesize vitamin C ~65 Ma since neither apes nor monkey nor tarsiers have a functional L-gulono-γ-lactone oxidase gene (Lachapelle and Drouin 2011). Our previous studies with resurrected uricases suggested that enzyme activity began to be catalytically reshaped some time between 96 and 43 Ma. The current study attempts to more accurately determine when this transition began by increasing the species diversity of the uricase phylogenetic tree, and thus increase the number of internal basal nodes for protein resurrection analysis.

In addition to understanding a correlation between uric acid build-up in apes with the loss of vitamin C synthesis in primates, our current study also attempts to determine whether ancient uricases may have potential value as therapeutic enzymes to prevent Tumor Lysis Syndrome and/or gouty arthritis in human patients (Najjari et al. 2021). As a

Article

step in this direction, ancient uricases are presented to a diverse panel of human immune-cell proliferation assays.

Results

Biomolecular Characterization of Resurrected Ancestral Uricases

The eutherian phylogeny inferred from uricase sequences has more than doubled in size over the past couple of years due to the Zoonomia Project (Zoonomia 2020). As seen in figure 1, these additional sequences provide greater resolution to a uricase phylogeny. In turn, such an increase in phylogenetic articulation can also provide greater accuracy in the inference of ancestral sequences at internal nodes of the tree (Hanson-Smith et al. 2010; Randall et al. 2016). We have resurrected ancient uricase enzymes along the evolutionary path that connect humans to their mammalian ancestors ~96 Ma. In agreement with our previous study, figure 1 demonstrates that ancient uricases were highly active enzymes that slowly and steadily decreased in activity until the enzyme became inactive in the lineage leading to apes ~20 Ma. The substrate affinity (K_m, fig. 2A), substrate turnover (K_{cat}, fig. 2B), and catalytic efficiency (K_{cat}/K_m, fig. 2C) were measured. A few results are worth highlighting. First, the catalytic efficiency of the enzyme slowly decreases from 96 to 29 Ma (fig. 2C, right side). This stepwise decrease results in 5-fold lower activity over 60 My. At this point along the evolutionary trajectory to apes, the enzyme is still overall highly active with an efficiency slightly less than the order of 10^5. Second, a precipitous decrease in enzyme activity occurs between 29 and 20 Ma (fig. 2C, left side). This decrease is caused by a single amino acid replacement (F222S) that results in complete loss of substrate turnover (Kratzer et al. 2014; Xie et al. 2016; Duan et al. 2021; Jiang et al. 2021). The phenylalanine at position 222 is located on helix $\alpha 4$ and stabilizes the dimer–dimer interface via aromatic stacking and hydrophobic interactions, and also has an intrasubunit cation–π interaction with the highly conserved Lys164. Replacement to serine eliminates these interactions and generates an energetic penalty by introducing a hydrophilic residue within this hydrophobic pocket. Since the four active sites of a homotetramer of uricase are the result of head-to-tail monomer/dimer interfaces, the enzyme no longer has stable active sites when serine occupies this position. Third, the last common ancestor of catarrhines (Old World monkey and apes, 29 Ma) had a uricase exhibiting very low substrate turnover (fig. 2B), and yet, its catalytic efficiency remained relatively robust because the improved K_m for substrate binding (by way of its lower value) is able to compensate for a lack of turnover. This same tradeoff in K_m and K_{cat} is maintained for the ancestor at ~12 Ma located within the Old World monkey clade (fig. 1) as well as the *Macaca mulatta* uricase we characterized ($K_m = 13.7$, $K_{cat} = 116$, $K_{cat}/K_m = 1.41 \times 10^5$). Conversely, the uricase of the New World monkey *Aotus nancymaae* that we characterized ($K_m = 22.1$, $K_{cat} = 266$, $K_{cat}/K_m = 2.01 \times 10^5$) more closely resembles An43 than An29. This observation is anticipated since the lineage is a direct descendent of node An43.

Immunogenicity of Ancestral Uricases

An immuno-cell proliferation assay was used to determine the relative antigenicity of ancestral uricases compared to a leading uricase therapeutic that forms the basis of the FDA-approved Krystexxa, which is a pig and baboon chimeric (PBC) (Anderson and Singh 2010; Hershfield et al. 2010). The dendritic-cell–T-cell (DC-T) assay utilized a panel of peripheral blood mononuclear cell samples from healthy human donors representing a diversity of 43 human leukocyte antigen (HLA) class II haplotypes. Figure 3 shows that PBC elicited the broadest immune response for the three uricases we assayed. This uricase stimulated >70% of HLA alleles represented in the assay. The An43 uricase fared better than PBC by stimulating just under 50% of the samples. The An96 uricase, however, performed best in the immunogenicity assay by stimulating only ~35% of the samples.

Lastly, we measured the stability of uricases in conditions that mimic the gastrointestinal tract of mammals to assess the potential oral delivery of a therapeutic uricase treatment (Szczurek et al. 2017; Yun et al. 2017; Pierzynowska et al. 2020). Initial creatinine stability assays included the *Candida* uricase, along with PBC and An96 enzymes. *Candida* was very unstable in these conditions, while PBC and An96 were highly stable (fig. 4). In attempt to further stabilize An96, we inserted disulfide bridges into the protein (Craig and Dombkowski 2013; Yainoy et al. 2019). One variant (Coel) had amino acid replacements at M25C and N287C, while a different variant (DbD3) had replacements at A223C and A130C. As seen in figure 4, one of the variants was markedly destabilized while the other variant was slightly more stable than An96 by the insertion of a disulfide bridge.

Discussion

Tracing the evolutionary history of uricases during placental mammalian evolution demonstrates that this enzyme experienced a slow and sequential reshaping over the course of ~70 My before its precipitous drop in activity by 20 Ma, crown group of apes. The slow decline in catalytic efficiency prior to apes was achieved by a balance of slower substrate turnover (decrease in K_{cat}) and weaker substrate binding (increase in K_m). The slow decline and reshaping of enzymatic activity would have allowed other components of the purine metabolism pathway to handle a modified flux of the small molecule. From a physiological perspective, such reshaping is reasonable since we know uricase-knockout mice/rats have a high mortality rate by 6 weeks postbirth due to complications from renal failure caused by hyperuricemia (Kelly et al. 2001). The mammalian body cannot handle a rapid and massive increase in uric acid caused by an abrupt lack of uricase activity. In support of this notion, our previous work with resurrected uric acid transporters demonstrated that the transporter URAT1 coevolved with the reshaping of uricase activity during mammalian evolution (fig. 5). Our current studies were able to add more uricase data points and thus provide greater resolution to the timing of the reshaping events. URAT1 evolved from a high-capacity/low-affinity transporter early in placental evolution to a low-capacity/

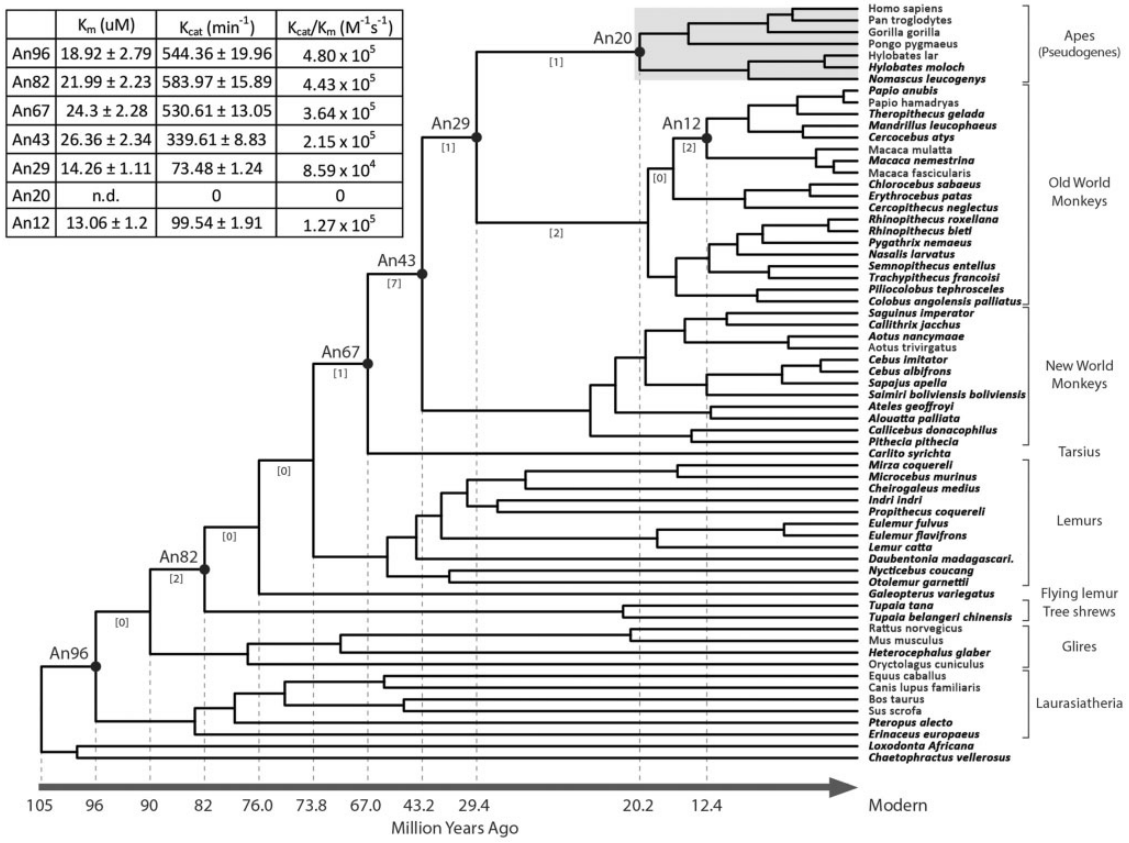

Fig. 1. Phylogenetic distribution of species used to infer ancestral uricase sequences. Species listed in bold font represent new sequences that were not included in our previous protein resurrection study (Kratzer et al. 2014). Geological timescale is calculated by TimeTree (Hedges et al. 2015). The number of amino acid replacements that occur along any given branch is provided in brackets below the branch. The inset table lists the biochemical properties of the resurrected uricase proteins listed in the phylogeny. The list of nonsynonymous substitutions that occurred along internal branches is provided in supplementary figure S6, Supplementary Material online.

high-affinity transporter by the predicted origins of the ape lineage (29 Ma). This transition is clearly in motion by 43 Ma as the capacity of the transporter was markedly decreasing while the affinity was conversely increasing, and is also accompanied by a notable decrease in uricase activity. The molecular events that occurred with uricase and URAT1 between 50 and 30 Ma clearly set the stage for the final blow to uricase activity shortly thereafter. The timing of these events suggest that the coevolution of uricase and URAT1 did not happen in direct response to the loss of vitamin C synthesis nearly 67 Ma.

While the chemical utility of uric acid as an antioxidant is indisputable, the physiological role for the presumed rise of endogenous uric acid 20 Ma in the crown apes is more speculative. We, along with others, have hypothesized that the increase in uric acid levels promote the biochemical conversion of fructose to triglycerides (Feig et al. 2008; Johnson et al. 2008, 2011, 2020; Johnson, Perez-Pozo, et al. 2009; Johnson, Sautin, et al. 2009; Johnson and Andrews 2010; Lanaspa et al. 2013; Lyssiotis and Cantley 2013; Choi et al. 2014; Cicerchi et al. 2014; Kratzer et al. 2014). The ability to ingest sucrose from fruits and immediately convert nearly half of the carbohydrate to a long-term storage molecule may have had a tremendous selective advantage for early apes and the increased energy demands required of their large brains compared to ancestral monkeys. We anticipate that additional future experiments will help resolve the precise evolutionary and physiological role of increased uric acid that originated nearly 20 Mya in apes.

Regardless of the true evolutionary cause of uricase deactivation, modern humans can suffer from an inability to properly manage endogenous uric acid levels. As such, pharmaceutical companies have spent decades attempting to develop recombinant uricases, as well as inhibitors of uric acid transporters. The race to develop a safe and effective therapeutic uricase has never been more competitive. The launch of Krystexxa (a PEGylated version of the PBC) nearly one decade ago has become a textbook case of failure. The fact that most human subjects elicit strong immune responses to the drug (Sundy et al. 2011; Lipsky et al. 2014; Nyborg et al. 2016), along with the fact that the FDA issued a black-box warning, meant most doctors were reluctant to prescribe and administer Krystexxa. The failure of the drug left a large gap in the gout/hyperuricemia market, so a flood of uricase variants/formulations are currently being developed. Krystexxa is being reformulated with an improved PEGylated moiety by 3SBIO (Shenyang, China). Selecta Biosciences (MA, USA) is encapsulating a PEGylated *Candida* uricases in viral particles in hopes of preventing an immune response in human patients (Kishimoto et al. 2016).

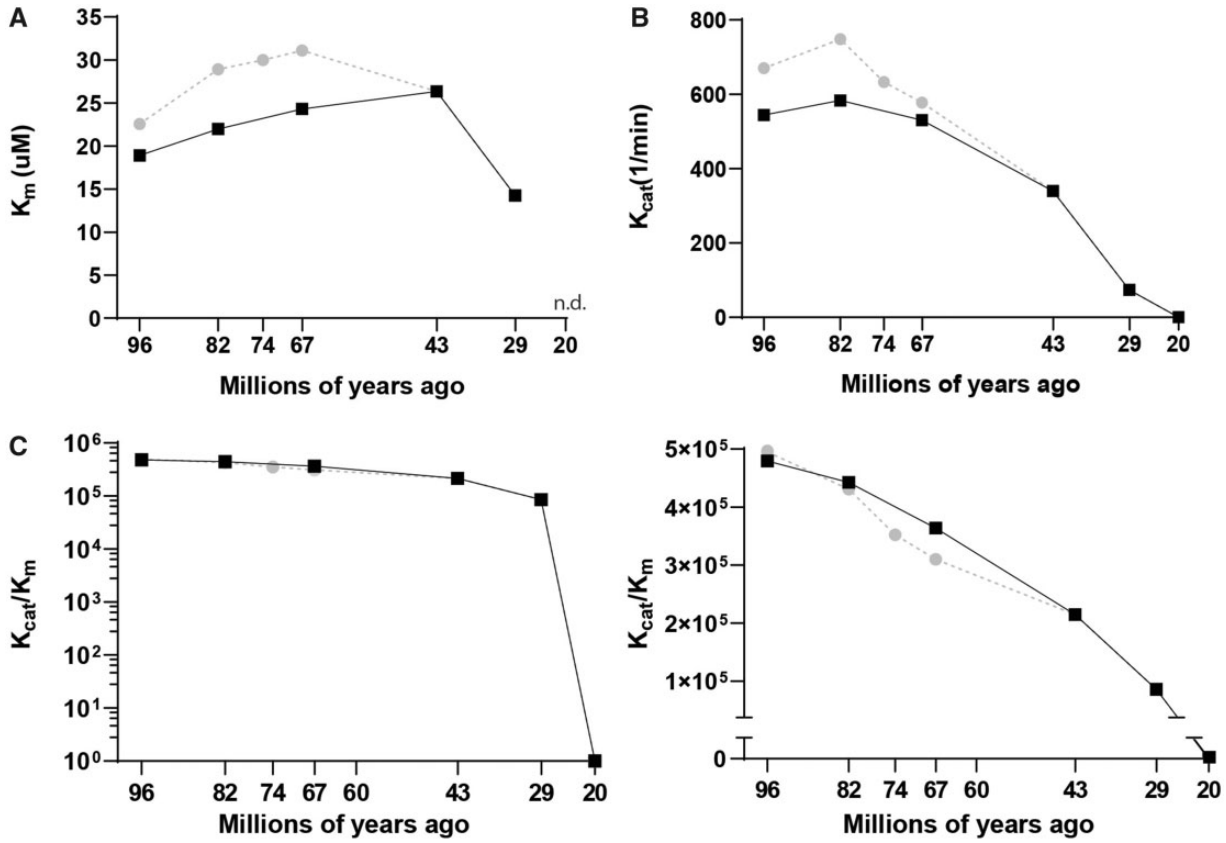

Fig. 2. The reshaping of uricase biomolecular properties over time. (*A*) Affinity of the uricase protein for uric acid substrate binding as described by the Michaelis constant (K_m). Lower values indicate stronger binding of the substrate. (*B*) The ability of the uricase protein to turnover (or oxidize) the uric acid substrate as a function of protein concentration and time (K_{cat}). (*C*) Catalytic efficiency measured as K_{cat}/K_m (logscale on the left, truncated scale on the right). Shown in the light gray are the biomolecular properties of ancestral enzymes inferred from nucleic acid sequences (instead of amino acid sequences) for nodes in which the DNA and protein inferences were not identical. The addition of so many species to our phylogeny (fig. 1) lead to different ancestral sequences compared to our previous study (Kratzer et al. 2014). Only An29 and An20 have identical sequences between the two studies. Regardless of the sequence differences for the other ancestral nodes between the two studies, it is evident that the biomolecular properties are nearly identical for corresponding nodes between the previous and current studies thereby supporting the robustness of the ancestral biomolecular properties at each node.

China Pharmaceutical University is engineering a uricase that essentially uses the resurrection approach to reactivate the human gene into a functional enzyme (Xie et al. 2016; Duan et al. 2021). Horizon Therapeutics (Dublin, Ireland) is currently coadministering the immune suppressor methotrexate along with PEGylated PBC uricase in clinical trials and demonstrated that patients have a lower immune response with this combination (Botson et al. 2021). In 2019, an academic research group reported that they engineered a uricase from the bacteria *Arthrobacter* that shows greater resistance to general protease digestion compared to other uricases (Shi et al. 2019). In 2020, Fagan Biomedical Inc. reported its development of a PEGylated canine uricase that has high bioavailability when presented to monkeys (Li et al. 2020).

There is clearly a lot of competition for a share of the gout/hyperuricemia market. There are two especially interesting developments that have recently occurred during this competition. Both of these developments involve an oral route for uricase delivery that exploits the discovery that the lower intestines play an important role is lowering serum uric acid levels (Yun et al. 2017). One approach uses *Staphylococcus* engineered to export uricase outside of a host bacterial cell. These bacteria have been gavaged (orally administered) in rats and shown to colonize the intestines and to release uricase and lower uric acid levels in the intestines (Cai et al. 2020). The other approach has engineered the *Candida* uricase to be hyperstable against the pH environment of the digestive tract. Animal studies have demonstrated that oral administration of this uricase can lower serum uric acid levels (Szczurek et al. 2017; Pierzynowska et al. 2020) and clinical studies in humans are currently being conducted by Allena Pharmaceuticals (MA, USA). Our results clearly demonstrate that ancestral uricases have superior stability compared to unmodified *Candida* and PBC uricases when assayed in conditions that simulate the mammalian gastrointestinal tract (fig. 4), and may thus serve as better potential therapeutics.

In total, these therapeutic developments led us to question how immunogenic ancestral proteins would be to human immune cells since these assays serve as a proxy for the safety of a potential therapeutic drug. Figure 3 demonstrates that our most ancestral uricase elicits a substantially lower

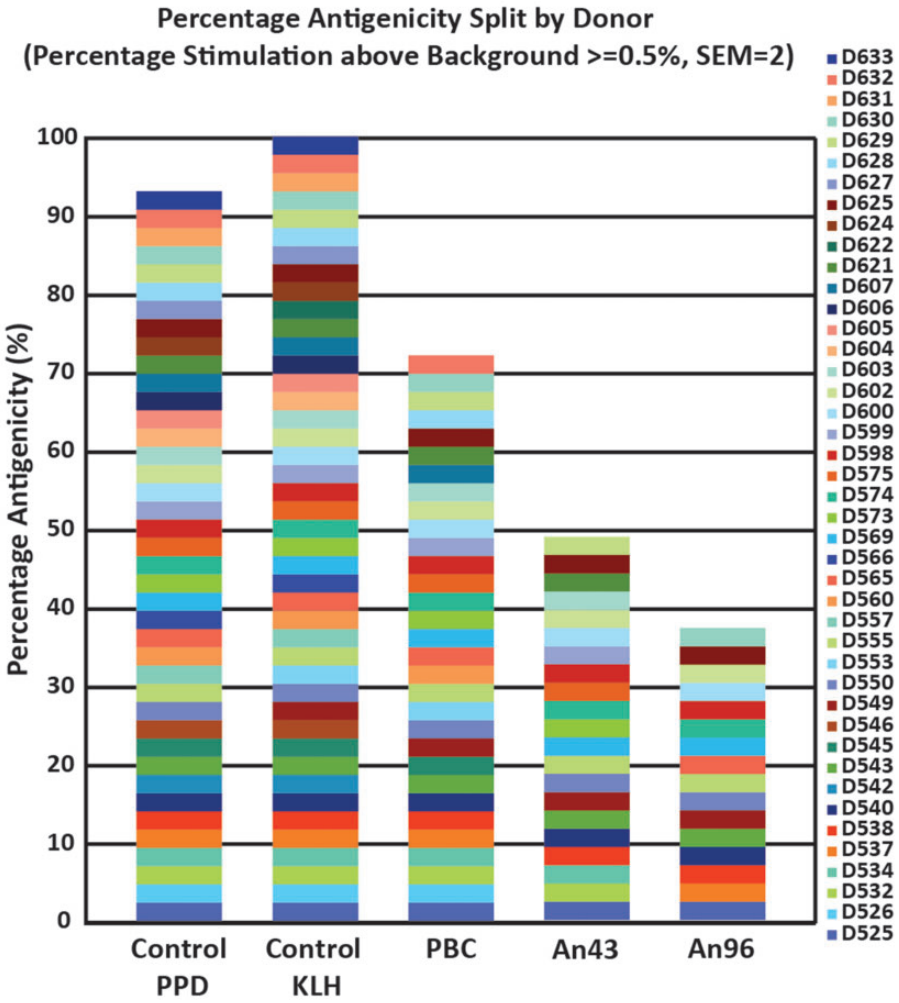

FIG. 3. Relative immunogenicity of ancestral and chimeric uricases against control proteins known to elicit strong immune responses from human dendritic cells. A panel of 43 HLA type II alleles was used to represent a diverse global pool.

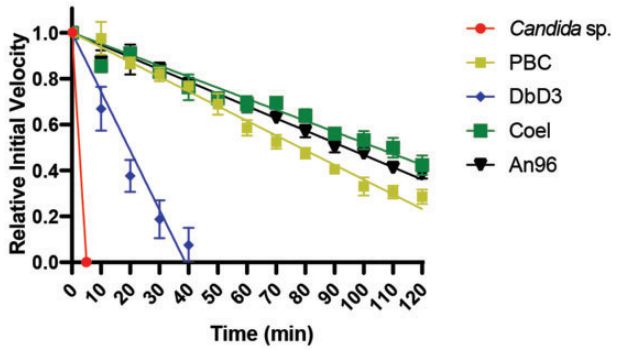

FIG. 4. The relative initial velocity of enzyme stability after incubation with pancreatin. The linear regression was performed and (absolute value of) slopes of the best-fit line in which each *y*-intercept is set at 1.0, which represent velocity of degradation, are presented in order of increasing stability: *Candida* yeast 0.2, DbD3 0.0257 (variant of An96), PBC 0.0064, An96 0.0053, and Coel 0.0048 (variant of An96).

immune response than the PBC uricase. PBC was initially developed from two observations: 1) monkey uricases are very unstable when purified (this is also true for both An29 and An12, but not other modern and ancestral uricases) and 2) clinical results showing that recombinant pig uricase elicited strong immune responses in human subjects supported the notion that incorporating portions of the monkey sequence into the pig sequence may diminish the immune response in human patients. This notion was highly speculative at the time, but appears to now be supported by the recent discovery of uricase protein expression based on human proteomic analyses (Na et al. 2019). The read-through of the two premature stop codons in the human transcript does not generate an enzymatically active protein as we demonstrated previously (Kratzer et al. 2014), but it may "teach" the human immune system that uricase-like peptides/proteins are benign. In total, our assays demonstrate that ancestral uricases are potentially advantageous compared to PBC. In fact, we would conclude that any therapeutic uricase that includes monkey sequence be abandoned because of its long evolutionary history with protein instability, and rather favor other ancestral uricases that are more stable and more human-like in sequence.

It is also noteworthy from these assays that An96 displayed a response index (RI) <0.7, which is comparable to other FDA-approved therapeutics such as Remicade, Avastin, Campath, and many others. Conversely, the RI for PBC was

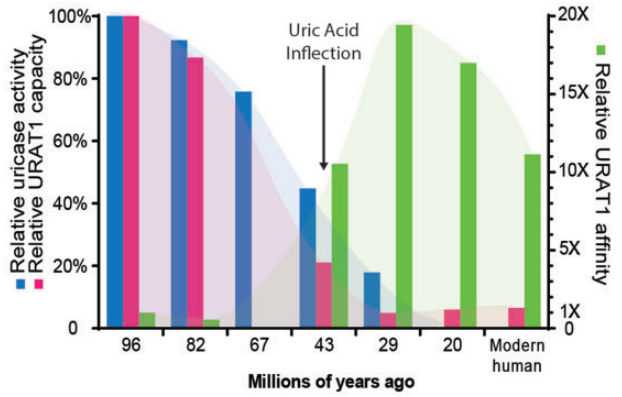

FIG. 5. Relationship between the reshaping of uricase and URAT1 during ancestral placental mammalian evolution leading to modern humans. This graph has been expanded from our previous studies (Tan et al. 2016). The biomolecular properties of the proteins appear to experience an inflection around 40 Ma and are completed by 20 Ma, the latter of which coincides with the origins of apes (Andrews 2020).

nearly 2.0 which is a warning sign that human immunogenicity will promote complications. With that said, additional experiments will determine whether ancestral uricases are truly useful for future therapeutic development.

To conclude, our results suggest that a substantial rise in endogenous uric acid levels coincided with the origins of ape species in the mammalian lineage 20–30 Ma and was independent of the loss of vitamin C synthesis that occurred in primates ~67 Ma. The rise in endogenous uric acid levels was preceded by a reshaping of the uricase enzyme and the uric acid transporter URAT1. While a growing repertoire of experimental results support one notion that increased levels of uric acid allowed apes to convert fructose to fatty acids, and thus served as a selective advantage, many additional experiments will be required before this hypothesis becomes parlance. We also anticipate that ancient uricases will support the growing idea of evolutionary biomedicine in the near future (Perry 2021; Selberg et al. 2021).

Materials and Methods

Representative DNA and protein sequences for uricase (E.C. 1.7.3.3) were identified from UniProtKB 2021_01 (https://www.uniprot.org/). Homologous DNA and protein sequences were retrieved from GenBank (https://www.ncbi.nlm.nih.gov/), using the nucleotide Basic Local Alignment Search Tool (nBLAST) and the protein BLAST (Altschul et al. 1990), respectively, with the cut-off threshold of $<1 \times 10^{-5}$. The majority of collected sequences were retrieved from species that were sequenced for the first time by the Zoonomia Project (Zoonomia 2020). These sequences were available only as genomic DNA sequences and thus BLAST searches were conducted against genomes (supplementary table S1, Supplementary Material online). Individual exon sequences were manually concatenated (supplementary fig. S4, Supplementary Material online). Assembled DNA sequences were translated into protein sequences using ExPASy (https://www.expasy.org/). Also, some of the retrieved protein sequences were found to contain superfluous intron sequences at the beginning of the Exon 1 sequence. These intron sequences were manually removed. In contrast, some of the retrieved protein sequences lacked portions of Exon 1. The automated annotation algorithm missed Exon 1 probably due to its short length. For species that had these shortened protein sequences, an inquiry sequence that combines a known Exon 1 sequence and an upstream intron sequence was manually prepared and utilized to find Exon 1 sequences by BLAST genome search. A total of 65 sequences were collected for further analysis.

Sequences were aligned using MUSCLE (ver. 3.8.31) (Edgar 2004). Taxon-specific insertions were manually removed. Trees were constructed using MrBayes (ver. 3.2.6) (Huelsenbeck et al. 2001), using the GTR+I+Γ model for the DNA sequences and the LG+I+Γ model for the protein sequences and run at least 1,000,000 generations, with sampling at intervals of 100 generations, and two runs with four chains per run in order to monitor convergence. Twenty-five percent of sampled points were discarded as burn-in. Tree topologies were nearly identical to the species tree published by the Zoonomia Project. When they differed, however, branches were manually edited using Mesquite (ver. 3.61) (supplementary figs. S2 and S3, Supplementary Material online). Ancestral sequences were reconstructed using PAML (ver. 4.8) (Yang 2007) as described previously (Kratzer et al. 2014) (supplementary fig. S5, Supplementary Material online). The average posterior probability across all sites for all ancestors we inferred (11 total) was greater than 99%.

Uricase-encoding genes were cloned into the pET-21a(+) vector (Life Technologies Corporation) using *Nde*I and *Xho*I sites. *Escherichia coli* BL21 (DE3; New England Biolabs) cells were freshly transformed with uricase-containing vectors. A single colony was used to inoculate a 5-ml overnight culture. This overnight culture was used to inoculate 500 ml of Luria Broth with 100 μg/ml carbenicillin. Cells were grown to an OD_{600} between 0.6 and 0.8 at which point they were induced with 1 mM IPTG. Expression was carried out overnight (16–20 h) at 37 °C with shaking at 250 rpm. After cells were harvested by centrifuge, the pellets were stored at −80 °C. The pellet was lysed and resuspended by 100% BugBuster protein extraction reagent (Novagen), followed by centrifugation. The lysate was washed with 55% and 10% BugBuster reagent, twice, respectively. The final pellet was resuspended in 0.1 M Na_2CO_3 buffer at pH 11 with 1 mM PMSF, followed by rocking for 60–90 min. Soluble uricases were purified using FPLC (Cytiva) at 4 °C and followed the two-step purification scheme described previously (Kratzer et al. 2014). The carbonate extraction was loaded on size-exclusion chromatography (HiLoad 16/60 Superdex 200 prep-grade column; Cytiva) preequilibrated with 0.1 M Na_2CO_3, pH 11. The protein with ~140 kDa was collected for anion exchange chromatography (SOURCE 15Q 4.6/100 PE [Cytiva]) preequilibrated with 0.1 M Na_2CO_3, pH 11. The sample was eluted in three different concentrations of NaCl diluted with 0.1 M Na_2CO_3 buffer (pH = 11): 0.15, 0.3, and 0.6 M. The concentration of purified tetrameric uricase was determined by the Quick Bradford Assay (Bio-Rad). Enzymatic curves for

all assayed enzymes are provided (supplementary fig. S1, Supplementary Material online).

The enzymatic activity of purified tetrameric uricase was determined spectrophotometrically by monitoring the decrease of uric acid by following the absorbance at 293 nm (A293). Using 96-well plate and platereader (Molecular Devices). A freshly prepared 200 μM uric acid stock in 1× sodium phosphate buffer, pH 7.4, was diluted with 1× sodium phosphate buffer (Gibco), pH 7.4, to prepare a range of uric acid concentrations from 0 to 150 μM.

The mean from triplicate runs of initial velocities at each uric acid concentration were used to plot a hyperbolic regression curve to determine K_m and V_{max} of the purified uricases (Graphpad Prism 9). The K_{cat} was determined by dividing V_{max} by the concentration of tetrameric uricase used in the kinetics experiments, and the catalytic efficiency (K_{cat}/K_m) was calculated by taking the ratio of K_{cat} to K_m.

Immunogenicity assays were conducted at ProImmune Ltd (Oxford, UK). Briefly, this DC-T proliferation assay helps to identify the presence or absence of potential T-cell epitopes within antigens. Cell proliferation is determined using the cell dye carboxyfluorescein succinimidyl ester (CFSE), which forms an intracellular fluorescent conjugate following cellular uptake. Fluorescence intensity of CFSE is halved through each consecutive cell division, thus allowing measurement of proliferation as a function of altered fluorescence of CFSE containing cells. Positive controls for cell proliferation include Tuberculin Purified Protein Derivative (PPD) and Keyhole Limpet Hemocyanin (KLH), to which donors are expected to respond through memory recall and naïve responses, respectively. The assay was performed by testing whole uricase proteins following our previous studies (Kratzer et al. 2014) against a set of 43 healthy human donor cell samples. Detection of proliferation of CD4+ T cells was performed by labeling cells with CFSE costaining with antihuman CD4 antibody. A panel of peripheral blood mononuclear cell (PBMC) samples was selected from the ProImmune cell bank. Each PBMC sample was HLA typed and stored in liquid nitrogen (vapor phase) prior to use. The panel was selected so that HLA class II alleles known to be highly expressed in the global population were well represented. Donors were predominantly selected by DRB1 allele expression. Alleles used to generate the data are available by request.

To measure stability of uricase against pancreatin, *Candida* sp. uricase (Sigma-Aldrich, U0880) and purified ancestral and PBC uricases were incubated with pancreatin: 0.25 mg/ml uricase was incubated with 2.5 mg/ml pancreatin (Sigma-Aldrich, P7545) at 37 °C. At indicated time points, 3 μl of the uricase: pancreatin mixture was added to 100 μM uric acid dissolved in simulated intestinal fluid (SIF) buffer (50 mM potassium phosphate, pH 6.8). The decrease in uric acid concentration was monitored by absorbance at 293 nm. The assay was performed at 37 °C. The linear regression was calculated with Graphpad Prism 9. The Disulfide by Design 2.0 webserver was used to predict the insertion of a single disulfide bridge into the uricase protein (Craig and Dombkowski 2013).

Supplementary Material

Supplementary data are available at *Molecular Biology and Evolution* online.

Acknowledgments

We thank Jennifer Farrar and James Kratzer for their technical assistance with sequence analyses and experiments. We also thank Richard Johnson and Miguel Lanaspa for their consultation. This work was supported by National Institutes of Health (R01AR069137), Human Frontier Science Program (RGP0041), National Science Foundation (2032315), and Department of Defense (MURI W911NF-16-1-0372).

Author Contributions

E.G. conceived the study, Y.H. performed the evolutionary analyses, Z.L. performed the biochemical assays, and L.T. generated the uricase variants for the stability assay. All authors contributed to the writing of the manuscript, and editing of the final manuscript. All authors approved the final version of the article.

Data Availability

All nucleic and amino acid sequences are available by request. Also, HLA allele information is available for the PBMCs used in the immunogenicity assay.

References

Altschul SF, Gish W, Miller W, Myers EW, Lipman DJ. 1990. Basic local alignment search tool. *J Mol Biol*. 215(3):403–410.

Ames BN, Cathcart R, Schwiers E, Hochstein P. 1981. Uric acid provides an antioxidant defense in humans against oxidant- and radical-caused aging and cancer: a hypothesis. *Proc Natl Acad Sci U S A*. 78(11):6858–6862.

Anderson A, Singh JA. 2010. Pegloticase for chronic gout. *Cochrane Database Syst Rev*. 2010(3):CD008335.

Andrews P. 2020. Last common ancestor of apes and humans: morphology and environment. *Folia Primatol*. 91(2):122–148.

Botson JK, Tesser JRP, Bennett R, Kenney HM, Peloso PM, Obermeyer K, LaMoreaux B, Weinblatt ME, Peterson J. 2021. Pegloticase in combination with methotrexate in patients with uncontrolled gout: a multicenter, open-label study (MIRROR). *J Rheumatol*. 48(5):767–774.

Cai LM, Li Q, Deng YB, Liu XJ, Du WH, Jiang X. 2020. Construction and expression of recombinant uricase-expressing genetically engineered bacteria and its application in rat model of hyperuricemia. *Int J Mol Med*. 45(5):1488–1500.

Choi YJ, Shin HS, Choi HS, Park JW, Jo I, Oh ES, Lee KY, Lee BH, Johnson RJ, Kang DH. 2014. Uric acid induces fat accumulation via generation of endoplasmic reticulum stress and SREBP-1c activation in hepatocytes. *Lab Invest*. 94(10):1114–1125.

Cicerchi C, Li N, Kratzer J, Garcia G, Roncal-Jimenez CA, Tanabe K, Hunter B, Rivard CJ, Sautin YY, Gaucher EA, et al. 2014. Uric acid-dependent inhibition of AMP kinase induces hepatic glucose production in diabetes and starvation: evolutionary implications of the uricase loss in hominids. *FASEB J*. 28(8):3339–3350.

Craig DB, Dombkowski AA. 2013. Disulfide by Design 2.0: a web-based tool for disulfide engineering in proteins. *BMC Bioinformatics*. 14:346.

Duan Y, Jiang N, Chen J, Chen J. 2021. Expression, localization and metabolic function of "resurrected" human urate oxidase in human hepatocytes. *Int J Biol Macromol*. 175:30–39.

Edgar RC. 2004. MUSCLE: multiple sequence alignment with high accuracy and high throughput. *Nucleic Acids Res*. 32(5):1792–1797.

Feig DI, Kang DH, Johnson RJ. 2008. Uric acid and cardiovascular risk. *N Engl J Med*. 359(17):1811–1821.
Hanson-Smith V, Kolaczkowski B, Thornton JW. 2010. Robustness of ancestral sequence reconstruction to phylogenetic uncertainty. *Mol Biol Evol*. 27(9):1988–1999.
Hedges SB, Marin J, Suleski M, Paymer M, Kumar S. 2015. Tree of life reveals clock-like speciation and diversification. *Mol Biol Evol*. 32(4):835–845.
Hershfield MS, Roberts LJ, Ganson NJ, Kelly SJ, Santisteban I, Scarlett E, Jaggers D, Sundy JS. 2010. Treating gout with pegloticase, a PEGylated urate oxidase, provides insight into the importance of uric acid as an antioxidant in vivo. *Proc Natl Acad Sci U S A*. 107(32):14351–14356.
Huelsenbeck JP, Ronquist F, Nielsen R, Bollback JP. 2001. Bayesian inference of phylogeny and its impact on evolutionary biology. *Science* 294(5550):2310–2314.
Jiang N, Xu C, Zhang L, Chen J. 2021. "Resurrected" human-source urate oxidase with high uricolytic activity and stability. *Enzyme Microb Technol*. 149:109852.
Johnson RJ, Andrews P. 2010. Fructose, uricase, and the back-to-Africa hypothesis. *Evol Anthropol*. 19(6):250–257.
Johnson RJ, Gaucher EA, Sautin YY, Henderson GN, Angerhofer AJ, Benner SA. 2008. The planetary biology of ascorbate and uric acid and their relationship with the epidemic of obesity and cardiovascular disease. *Med Hypotheses*. 71(1):22–31.
Johnson RJ, Lanaspa MA, Gaucher EA. 2011. Uric acid: a danger signal from the RNA world that may have a role in the epidemic of obesity, metabolic syndrome, and cardiorenal disease: evolutionary considerations. *Semin Nephrol*. 31(5):394–399.
Johnson RJ, Perez-Pozo SE, Sautin YY, Manitius J, Sanchez-Lozada LG, Feig DI, Shafiu M, Segal M, Glassock RJ, Shimada M, et al. 2009. Hypothesis: could excessive fructose intake and uric acid cause type 2 diabetes? *Endocr Rev*. 30(1):96–116.
Johnson RJ, Sautin YY, Oliver WJ, Roncal C, Mu W, Gabriela Sanchez-Lozada L, Rodriguez-Iturbe B, Nakagawa T, Benner SA. 2009. Lessons from comparative physiology: could uric acid represent a physiologic alarm signal gone awry in western society? *J Comp Physiol B*. 179(1):67–76.
Johnson RJ, Stenvinkel P, Andrews P, Sanchez-Lozada LG, Nakagawa T, Gaucher E, Andres-Hernando A, Rodriguez-Iturbe B, Jimenez CR, Garcia G, et al. 2020. Fructose metabolism as a common evolutionary pathway of survival associated with climate change, food shortage and droughts. *J Intern Med*. 287(3):252–262.
Keebaugh AC, Thomas JW. 2010. The evolutionary fate of the genes encoding the purine catabolic enzymes in hominoids, birds, and reptiles. *Mol Biol Evol*. 27(6):1359–1369.
Kelly SJ, Delnomdedieu M, Oliverio MI, Williams LD, Saifer MG, Sherman MR, Coffman TM, Johnson GA, Hershfield MS. 2001. Diabetes insipidus in uricase-deficient mice: a model for evaluating therapy with poly(ethylene glycol)-modified uricase. *J Am Soc Nephrol*. 12(5):1001–1009.
Kishimoto TK, Ferrari JD, LaMothe RA, Kolte PN, Griset AP, O'Neil C, Chan V, Browning E, Chalishazar A, Kuhlman W, et al. 2016. Improving the efficacy and safety of biologic drugs with tolerogenic nanoparticles. *Nat Nanotechnol*. 11(10):890–899.
Kratzer JT, Lanaspa MA, Murphy MN, Cicerchi C, Graves CL, Tipton PA, Ortlund EA, Johnson RJ, Gaucher EA. 2014. Evolutionary history and metabolic insights of ancient mammalian uricases. *Proc Natl Acad Sci U S A*. 111(10):3763–3768.
Lachapelle MY, Drouin G. 2011. Inactivation dates of the human and guinea pig vitamin C genes. *Genetica* 139(2):199–207.
Lanaspa MA, Ishimoto T, Li N, Cicerchi C, Orlicky DJ, Ruzycki P, Rivard C, Inaba S, Roncal-Jimenez CA, Bales ES, et al. 2013. Endogenous fructose production and metabolism in the liver contributes to the development of metabolic syndrome. *Nat Commun*. 4:2434.
Li H, Huo J, Sun D, Jiang L, Hu C, Bai Y, Ma X, Zhang H, Shi X, Zhao Z, et al. 2020. Pharmacokinetics of polyethylene glycol-modified canine uricase following single and multiple intravenous injections in cynomolgus monkeys. *Eur J Drug Metab Pharmacokinet*. 45(4):445–451.
Lipsky PE, Calabrese LH, Kavanaugh A, Sundy JS, Wright D, Wolfson M, Becker MA. 2014. Pegloticase immunogenicity: the relationship between efficacy and antibody development in patients treated for refractory chronic gout. *Arthritis Res Ther*. 16(2):R60.
Lyssiotis CA, Cantley LC. 2013. Metabolic syndrome: F stands for fructose and fat. *Nature* 502(7470):181–182.
Na CH, Sharma N, Madugundu AK, Chen R, Aksit MA, Rosson GD, Cutting GR, Pandey A. 2019. Integrated transcriptomic and proteomic analysis of human eccrine sweat glands identifies missing and novel proteins. *Mol Cell Proteomics*. 18(7):1382–1395.
Najjari A, Shahbazmohammadi H, Omidinia E, Movafagh AM. 2021. The effective control of hyperuricemia in cancer patients: a new recombinant conjugated variant of urate oxidase. *Asian Pac J Cancer Prev*. 22(2):627–632.
Nyborg AC, Ward C, Zacco A, Chacko B, Grinberg L, Geoghegan JC, Bean R, Wendeler M, Bartnik F, O'Connor E, et al. 2016. A therapeutic uricase with reduced immunogenicity risk and improved development properties. *PLoS One*. 11(12):e0167935.
Perry GH. 2021. Evolutionary medicine. *Elife* 10:e69398.
Pierzynowska K, Deshpande A, Mosiichuk N, Terkeltaub R, Szczurek P, Salido E, Pierzynowski S, Grujic D. 2020. Oral treatment with an engineered uricase, ALLN-346, reduces hyperuricemia, and uricosuria in urate oxidase-deficient mice. *Front Med*. 7:569215.
Ramazzina I, Folli C, Secchi A, Berni R, Percudani R. 2006. Completing the uric acid degradation pathway through phylogenetic comparison of whole genomes. *Nat Chem Biol*. 2(3):144–148.
Randall RN, Radford CE, Roof KA, Natarajan DK, Gaucher EA. 2016. An experimental phylogeny to benchmark ancestral sequence reconstruction. *Nat Commun*. 7:12847.
Selberg AGA, Gaucher EA, Liberles DA. 2021. Ancestral sequence reconstruction: from chemical paleogenetics to maximum likelihood algorithms and beyond. *J Mol Evol*. 89(3):157–164.
Shi Y, Wang T, Zhou XE, Liu QF, Jiang Y, Xu HE. 2019. Structure-based design of a hyperthermostable AgUricase for hyperuricemia and gout therapy. *Acta Pharmacol Sin*. 40(10):1364–1372.
Sundy JS, Baraf HS, Yood RA, Edwards NL, Gutierrez-Urena SR, Treadwell EL, Vazquez-Mellado J, White WB, Lipsky PE, Horowitz Z, et al. 2011. Efficacy and tolerability of pegloticase for the treatment of chronic gout in patients refractory to conventional treatment: two randomized controlled trials. *JAMA* 306:711–720.
Szczurek P, Mosiichuk N, Woliński J, Yatsenko T, Grujic D, Lozinska L, Pieszka M, Święch E, Pierzynowski SG, Goncharova K. 2017. Oral uricase eliminates blood uric acid in the hyperuricemic pig model. *PLoS One*. 12(6):e0179195.
Tan PK, Farrar JE, Gaucher EA, Miner JN. 2016. Coevolution of URAT1 and uricase during primate evolution: implications for serum urate homeostasis and gout. *Mol Biol Evol*. 33(9):2193–2200.
Wells HG. 1910. The relation of fatty degeneration to the oxidation of purines by liver cells. *J Exp Med*. 12(5):607–615.
Xie G, Yang W, Chen J, Li M, Jiang N, Zhao B, Chen S, Wang M, Chen J. 2016. Development of therapeutic chimeric uricase by exon replacement/restoration and site-directed mutagenesis. *Int J Mol Sci*. 17(5):764.
Yainoy S, Phuadraksa T, Wichit S, Sompoppokakul M, Songtawee N, Prachayasittikul V, Isarankura-Na-Ayudhya C. 2019. Production and characterization of recombinant wild type uricase from Indonesian coelacanth (*L. menadoensis*) and improvement of its thermostability by in silico rational design and disulphide bridges engineering. *Int J Mol Sci*. 20(6):1269.
Yang Z. 2007. PAML 4: phylogenetic analysis by maximum likelihood. *Mol Biol Evol*. 24(8):1586–1591.
Yun Y, Yin H, Gao Z, Li Y, Gao T, Duan J, Yang R, Dong X, Zhang L, Duan W. 2017. Intestinal tract is an important organ for lowering serum uric acid in rats. *PLoS One*. 12(12):e0190194.
Zoonomia C. 2020. A comparative genomics multitool for scientific discovery and conservation. *Nature* 587:240–245.